

FIG. 10. Variation of $|\chi_3 - \chi_1|$ with atomic percentage of antimony at room temperature.

$\times 100$ would be about 0.2 percent in the 0.12 atomic percent Sb sample, for example, and would not be detectable in the data.

The large change in $\chi_3 - \chi_1$ at room temperature with a very small increase of Sb in the Sn indicates that the added electrons go into a more or less localized region in k space, removed from the regions responsible for the de Haas-van Alphen effect, rather than distribute themselves uniformly over the entire Fermi surface.

A tentative explanation of the variation of X with ϕ is as follows: The parameter X is a function of the reciprocal of the mean free time between collisions for the de Haas-van Alphen electrons. This is demonstrated by Fig. 5, which shows that as the number of Sb atoms in Sn increases, thereby increasing the number of scattering centers, X increases. Since theoretical con-

siderations show that the electron motion in the plane perpendicular to the field is responsible for the de Haas-van Alphen effect, it therefore seems plausible that as the angle between the field and the tetragonal axis of the sample is increased, the plane of the orbits of the de Haas-van Alphen electrons rotates into a more densely packed plane of atoms, which gives rise to shorter mean free times, therefore larger values of X . It is interesting that the value of X at $\phi \cong 30^\circ$ is about three or four times the value of X between 0° and 20° . The de Haas-van Alphen electrons would be rotating in the (101) plane at $\phi = 28.5^\circ$. This plane is more densely packed than the 100 plane in Sn.

The small value of X for pure tin is attributed to the fact that great care was taken to avoid straining the crystal in any way and to the heat treatment given the sample.

At first sight, one might think that the nonlinearity of the $\log_{10}(aH^3)$ vs H^{-1} plots is due to failure to include sufficient terms of the series given in Eq. (3). A calculation of the contribution of the second term, at a reasonable field strength and temperature, to the amplitude shows that it is too small to account for the observed deviations.

It appears that a higher power of H than $3/2$ would give a better fit to the experimental results.

Neutron Diffraction Studies of a Nickel Zinc Ferrite*

V. C. WILSON AND J. S. KASPER
General Electric Research Laboratory, Schenectady, New York

(Received June 8, 1954)

Neutron diffraction studies have been made of a ferrite powder of composition $Zn_{0.5}Ni_{0.5}Fe_2O_4$. The crystal structure is of the spinel type with 4 Zn^{++} and 4 Fe^{+++} ions in the tetrahedral positions and 4 Ni^{++} and 12 Fe^{+++} ions in the octahedral positions. The magnetic structure at $25^\circ C$ appears to have an antiparallel arrangement of the Fe^{+++} spins on the two sites and a random orientation of the Ni^{++} spins.

INTRODUCTION

RECENT neutron diffraction studies of ferrites¹⁻⁴ have clearly demonstrated the special advantages of neutron diffraction for determining both the chemical and magnetic structures of these substances. Thus, while with x-rays it is difficult to ascertain the distribution of the respective cations and even more difficult to obtain a precise value of the oxygen parameter, the use of neutrons readily provides both kinds of information. Even more important is the opportunity by

means of neutron diffraction to obtain directly the location and magnitude of atomic magnetic moments. In the case of $ZnFe_2O_4$ and $NiFe_2O_4$ ² the findings are in agreement with prior postulates as to both the distribution of the ions and the magnetic structures.^{5,6} Thus, $ZnFe_2O_4$ is of the normal spinel type with no magnetic moment alignment, and $NiFe_2O_4$ is of the inverted type with the ferrimagnetic structure proposed by Néel.⁶ It is of interest to ascertain whether the same postulates apply to a ferrite containing both Zn and Ni. The present study was made for this purpose with a specimen of composition $Ni_{0.5}Zn_{0.5}Fe_2O_4$.

* The observations were made at the Brookhaven National Laboratory.

¹ Shull, Wollan, and Koehler, Phys. Rev. **84**, 912 (1951).

² J. M. Hastings and L. M. Corliss, Revs. Modern Phys. **25**, 114 (1953).

³ Corliss, Hastings, and Brockman, Phys. Rev. **90**, 1013 (1953).

⁴ G. E. Bacon and F. F. Roberts, Acta Cryst. **6**, 57 (1953).

⁵ E. J. W. Verwey and E. L. Heilmann, J. Chem. Phys. **15**, 174 (1947).

⁶ L. Néel, Ann. Physik **3**, 137 (1948).

EXPERIMENTAL PROCEDURE

The ferrite was prepared according to the reaction $0.5\text{NiO} + 0.5\text{ZnO} + \text{Fe}_2\text{O}_3 \rightarrow \text{Ni}_{0.5}\text{Zn}_{0.5}\text{Fe}_2\text{O}_4$. The components were pure powders intimately mixed in a colloid mill using distilled water. The water was then evaporated in an oven at 120°C and the resulting cake was pulverized and screened through a 30 mesh screen. This material was fired in air in mullite boats for 4 hours at 1350°C and furnace cooled. The x-ray diffraction pattern of the product corresponded to a spinel structure, which accounted for all the lines that were observed.

A bar of the ferrite was made from the same powder mixture and fired at the same temperature as the powder sample. The magnetic saturation for this bar was 4260 gauss which corresponds to 3.0 Bohr magnetons per formula $\text{Ni}_{0.5}\text{Zn}_{0.5}\text{Fe}_2\text{O}_4$. Guillaud⁷ reports an extrapolated value of 5.4 Bohr magnetons per molecule at absolute zero; therefore, a value of 3 Bohr magnetons seems reasonable at room temperature.

For the neutron diffraction experiments, the powdered product was sieved through 100 mesh screen and loosely packed into a flat cell of dimensions $\frac{1}{2}$ in. \times $2\frac{1}{4}$ in. \times 4 in.

TABLE I. Observed parameters.^a

	Nickel	Ferrite at 338°C	Ferrite at 25°C
a_0	3.524 Å	8.43 Å	8.38 Å
h	1.29 cm	1.37 cm	1.37 cm
ρ'	5.736 g/cm ³	2.54 g/cm ³	2.59 g/cm ³
$e^{-\mu h}$	0.227	0.624	0.597

^a $P_{111}(\text{nickel}) = 1513$ (arbitrary scale), $F_{111}^2 = 17.11$.

The two large surfaces of the cell were of thin boron-free glass. The $\frac{1}{2}$ -in. thick specimen was set in the transmission arrangement and was irradiated with a 2-in. square beam of neutrons of 1.05 Å wavelength. The "monochromatic" beam was obtained by reflection of the neutron source from a (200) face of a large lead crystal. Collimation was accomplished by means of Soller slits, and the diffracted rays were detected by a BF_3 proportional counter. A detailed description of the apparatus is to be published elsewhere.⁸

The diffracted intensity was recorded at intervals of $10'$ of arc. The number of diffracted neutrons was recorded for a fixed number of incident neutrons on the sample as determined by a beam monitor counter. Integrated intensities were determined by measuring with a planimeter the areas under the peaks and were placed on an "absolute" basis by reference to the area of a (111) peak of Ni. For the calculations the following expression, appropriate for the integrated power of a diffraction peak obtained in transmission through a

⁷ C. Guillaud, J. phys. et radium **12**, 244 (1951).

⁸ Wilson, Roberts, Geisler, Kasper, and Roth, Rev. Sci. Instr. (to be published).

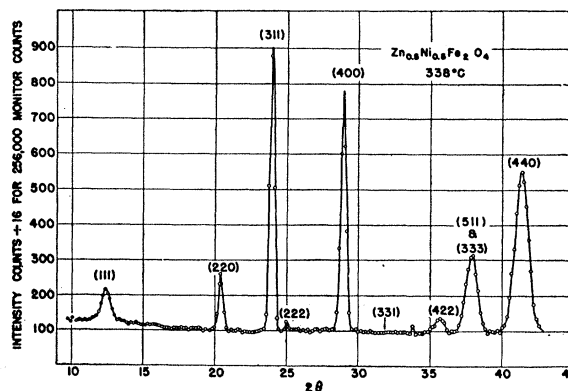


FIG. 1. Neutron diffraction pattern of a 50-50 nickel-zinc ferrite at 338°C .

cell, was used:

$$P_{hkl} = \left(P_0 \lambda^3 \frac{l}{4\pi r} \right) \left(N^2 h \frac{\rho'}{\rho} \right) \left(\frac{e^{-\mu h \sec \theta}}{\sin^2 2\theta} \right) T g J_{hkl} F_{hkl}^2, \quad (1)$$

where P_0 = number of neutrons striking the sample in unit time, λ = neutron wavelength, l = counter slit height, r = distance from counter slit to sample, N = number of unit cells per cm³, h = thickness of sample, ρ' = apparent density of powder, ρ = density of solid crystal, μ = effective linear absorption coefficient, T = temperature correction = $\exp[-2B(\sin\theta/\lambda)^2]$, g = geometrical correction factor for thick samples, J_{hkl} = multiplicity, and F_{hkl} = the structure factor.

The quantity $e^{-\mu h}$ was determined directly by measuring the transmission through the sample at $\theta = 0$. The geometrical factor, g , is a special one for the conditions of our experimental arrangement. Its derivation is given in the appendix.

In normalizing to a nickel reflection the terms in the first bracket drop out. Table I gives the observed quantities necessary for application of Eq. (1).

CRYSTAL STRUCTURE

For $\text{Ni}_{0.5}\text{Zn}_{0.5}\text{Fe}_2\text{O}_4$, the structure determination consists of ascertaining the distribution of the three metal ions among the positions $8a$ (tetrahedral) and $16d$ (octahedral) of space group $Fd\bar{3}m - O_h^7$, and of a

TABLE II. Intensities at 338°C for $\text{Zn}_{0.5}\text{Ni}_{0.5}\text{Fe}_2\text{O}_4$.

hkl	Observed	Calculated
111	155	149
220	113	139
311	643	653
222	14	10
400	603	601
331	0	3
422	75	72
511	408	449
333		
440	1001	1085

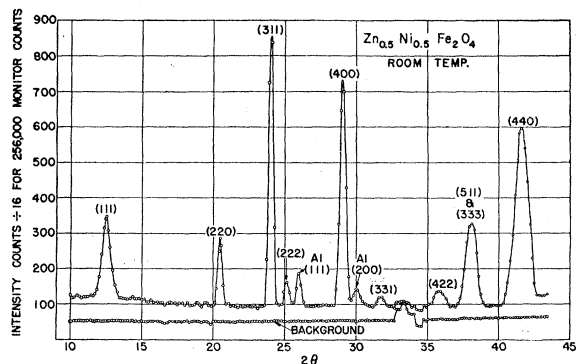


FIG. 2. Neutron diffraction pattern of a 50-50 nickel-zinc ferrite at room temperature.

determination of the oxygen parameter, u . The diffraction data at 338°C shown in Fig. 1 were used primarily for this purpose. Since the Curie temperature of this material is 260°C, it was assumed that at 338°C no magnetic contribution was present in any of the observed peaks.

The best fit of the calculated to the observed intensities was obtained for a model in which the tetrahedral positions were filled with 4 Zn^{++} ions and 4 Fe^{+++} ions distributed at random and that the octahedral positions were occupied by 12 Fe^{+++} ions and 4 Ni^{++} ions also distributed at random. In this case the best value for u was 0.383 ± 0.002 (see Table II). For these calculations a Debye-Waller temperature correction was used with the constant $B = 1.4 \times 10^{-8}$ which corresponds to a characteristic temperature of 385°K. The following values of the nuclear scattering amplitudes were used:

$$b_{Ni} = 1.03 \times 10^{-12} \text{ cm}; \quad b_{Zn} = 0.59 \times 10^{-12} \text{ cm};$$

$$b_{Fe} = 0.96 \times 10^{-12} \text{ cm}; \quad b_{oxygen} = 0.58 \times 10^{-12} \text{ cm}.$$

Among other models that were considered were those wherein (a) the separate ions are ordered in tetrahedral or octahedral sites, or both; and (b) there is a partial inversion (some Ni^{++} in tetrahedral, some Zn^{++} in octahedral sites). None of these models was as satisfactory as the one above, regardless of the parameter value u .

MAGNETIC STRUCTURE

The diffraction pattern obtained at room temperature (25°C) is shown in Fig. 2. At this temperature for the most part there is superposition of magnetic and nuclear intensities. Only the (331) reflection appears to be purely magnetic. The nuclear intensities can be expected to differ from those at 338°C because of a different temperature factor and perhaps a slightly different u parameter. It was assumed that u remained at 0.383. The nuclear intensities at room temperature were obtained by correcting the observed intensities of the lines at 338°C to the value they would have without the Debye-Waller temperature effect, then by applying

to these data a new temperature factor appropriate to room temperature. These results are shown in column 3 of Table III. The observed intensities are in column 4 and the difference between columns 4 and 3 gives the magnetic intensity, column 5.

Several arrangements and orientations of the magnetic ions were considered and F^2 values determined for each arrangement. To calculate F values it was assumed that an Fe^{+++} ion has 5 Bohr magnetons and a scattering amplitude of 1.35×10^{-12} cm; Ni^{++} , 2 Bohr magnetons, and 0.54×10^{-12} cm. In this case, $F^2 = F_{nuc}^2 + f^2 q^2 F_{mag}^2$, where f is the form factor given by Corliss and Hastings,² and q is the factor relating the orientation of the magnetic moment of the scattering particle to the orientation of the scattering plane. For a powder sample with cubic symmetry and with no magnetic field applied $q^2 = \frac{2}{3}$ for all diffracted lines. The five arrangements that most nearly fitted the observed data are shown as cases I to V of Table III. In these five cases it was assumed that any magnetic alignment in a tetrahedral site was 180° to any alignment in the

TABLE III. Magnetic intensities for $Zn_{0.5}Ni_{0.5}Fe_2O_4$.

<i>hkl</i>	Obs. nucl. 338°C	Nucl. 25°C	Obs. 25°C	Diff. = mag. obs.	Calculated magnetic				
					I	II	III	IV	V
111	155	157	332	175	136	263	164	305	294
220	113	118	156	38	9	38	13	38	33
311	643	668	671	3	12	4	11	8	10
222	14	15	66	51	39	51	44	66	68
400	603	657	690	33	30	55	36	65	64
331	0	0	34	34	27	53	33	61	59
422	75	85	82	-3	3	12	5	12	10
511	408	472	468	-4	3	4	2	1	2
333									
440	1001	1200	1193	-7	3	2	4	4	5

octahedral sites. Except in case V, considerations were given only to arrangements that would yield a net magnetic moment of 3 Bohr magnetons per molecule. As at 338°C, it was assumed that for each unit cell 4 Fe^{+++} ions were in the tetrahedral sites, $8a$, and 12 Fe^{+++} and 4 Ni^{++} ions were in the octahedral sites, $16d$. Case I is for one-half the magnetic spins lined up in both sites. Case II is for the iron in the $8a$ sites perfectly oriented and the Ni and Fe in the $16d$ sites both 0.647 oriented. Case III is for the Fe in $8a$ and $16d$ 0.6 oriented, Ni not oriented. Case IV is for Fe in $8a$ perfectly oriented, Fe in $16d$ 0.733 oriented, Ni not oriented. As before, the calculated intensities are in reference to the Ni-powder standard.

Niessen⁹ has published a theoretical treatment to calculate the spontaneous magnetization of the nickel zinc ferrites. Using his equations one would expect that at room temperature a 50-50 Ni-Zn ferrite would have 3.26 Bohr magnetons per molecule, and the average moments of the ions would be: Fe^{+++} in $8a$, 4.65 Bohr magnetons; Fe^{+++} in $16d$, 3.24 Bohr magnetons; and

⁹ K. F. Niessen, *Physica* 18, 449-468 (1952).

Ni²⁺ in 16*d*, 1.44 Bohr magnetons. Case V is the calculation of the neutron diffraction intensities to be expected for this distribution.

It appears that model III (Fe 0.6 lined up and Ni not lined up) gives the best fit with observed intensities, though some of the other models, notably I, cannot be ruled out. Except for (220), the agreement is quite satisfactory for III. The value of 38 (column 5), obtained by the difference procedure for (220), may well be quite too high, resulting from a too low value for the nuclear contribution at 338°C, as can be seen with reference to Table III. Attaching most weight to (111), (222), and (331), which are least sensitive to the nuclear contributions, model III would be definitely favored.

Additional support for model III is given by a comparison of the calculated and observed total intensities at 25°C (Table IV).

CONCLUSIONS

The arrangement of the metal ions is as one would predict from Verwey's observations on the family of

TABLE IV. Total intensities (nuclear+magnetic) at 25°C.

<i>hkl</i>	Observed	Calculated				
		I	II	III	IV	V
111	332	285	412	313	454	444
220	156	150	179	154	179	173
311	671	695	687	694	691	693
222	66	50	61	54	76	78
400	690	669	693	675	703	702
331	34	30	56	36	64	62
422	82	82	91	84	91	89
511	468	511	512	511	510	510
333						
440						
440	1193	1273	1271	1273	1273	1274

ferrites. The antiparallel arrangement of the iron spins on the 8*a* and 16*d* sites was predicted by the Néel theory; however, the apparent lack of lineup of the nickel magnetic moments is a little surprising. The theories are not sufficiently well developed to rule out this possibility.

APPENDIX I

Geometric Correction Factor, *g*

The monochromatic incident neutron beam striking the sample has a cross section of 2 in. by 2 in. The BF₃

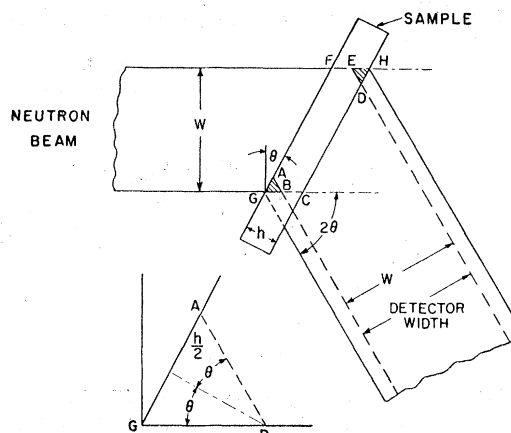


FIG. 3. Diagram for calculating geometric correction factor.

proportional counter detector has a solar slit system before it so that the effective cross section of the detector is also 2 in. by 2 in. From Fig. 3 one can see that the neutrons scattered in the direction 2θ from the two small shaded areas will pass outside the detector. Equation (1) of this paper is based upon the assumption that all the neutrons diffracted by the sample are detected. Therefore, a correction factor must be used which is the ratio of the area *ABCDEF* to the area *GCHF*. The sample is rotated to an angle θ when the detector arm is rotated to an angle 2θ from the axis of the beam. If *W* is the width of the beam and the detector and *h* is the thickness of the sample, then

$$g = \frac{\text{area } ABCDEF}{\text{area } GCHF} = \frac{\text{area } GCHF - 2 \text{ area } GAB}{\text{area } GCHF},$$

$$g = \frac{hW/\cos\theta - 2(t/2 \times t/2 \tan\theta)}{hW/\cos\theta},$$

$$g = 1 - \frac{h \sin\theta}{2W}.$$

In the case $h = \frac{1}{2}$ in. and $W = 2$ in., we therefore obtain $g = 1 - \frac{1}{8} \sin\theta$.